Heat Transfer Engineering, 29(9):774–781, 2008
Copyright © Taylor and Francis Group, LLC
ISSN: 0145-7632 print / 1521-0537 online
DOI: 10.1080/01457630802053777

Taylor & Francis
Taylor & Francis Group

Experimental and Numerical Investigation of a Microjet-Based Cooling System for High Power LEDs

XIAOBING LUO,[1] WEI CHEN,[1] RENXIA SUN,[1] AND SHENG LIU[2]

[1]School of Energy and Power Engineering, Huazhong University of Science & Technology, Wuhan, China
[2]Institute for Microsystems, Huazhong University of Science & Technology, Wuhan, China

The optical extraction efficiency and reliability of light emitting diodes (LEDs) relies heavily on successful thermal management due to their inherit dependence on the low junction temperature of LED chips. In this paper, a microjet-based cooling system is proposed for the thermal management of high power LEDs. Experimental and numerical investigations on such an active cooling system were conducted. Thermocouples were packaged with LED chips to conduct an online measurement of the temperature and evaluate the cooling performance of the proposed system. The experimental results demonstrate that the microjet-based cooling system has good cooling performance. For a 2×2 LED chip array, when the input power is 5.6 W and the environmental temperature is 28°C, the temperature of the 2×2 LED chip array reaches 72°C within 2 minutes and continues to increase sharply if no active cooling technique is applied. By using the proposed cooling system to cool the LEDs, however, the maximum LED temperature measured by thermocouples will remain stable at about 36.7°C, when the flow rate of the micropump is 9.7 mL/s. With consideration of the experimental difficulty, a numerical investigation was conducted on flow and temperature distribution in the microjet device. The feasibility of the numerical model was proven by comparison with experimental results. The numerical results showed that at a flow rate of 3.2 mL/s, the heat transfer coefficient of the impinging jets in the proposed system was about 5523 W/m^2·K, and the pressure drop in the microjet device was about 1368 Pa.

INTRODUCTION

Light-emitting diodes (LEDs) have received much attention in recent years because of their advantages compared with traditional light sources. Two examples of the traditional light sources are incandescent filament lamps and fluorescent lamps. Both of these are associated with large energy losses that are essentially inherent because of high temperatures and the large Stokes shifts involved [1]. LEDs depend on semiconductor materials to emit the light. Theoretically, they have many distinctive advantages such as high efficiency, good reliability, long life, variable color, and low power consumption. Recently, LEDs have begun to play an important role in many applications [2]. Typical applications include back lighting for cell phones and other LCD displays; interior and exterior automotive lighting, including headlights; large signs and displays; signals; and illumination. LEDs will soon be used in general lighting such as street lights.

Address correspondence to Professor Sheng Liu, Institute for Microsystems, Huazhong University of Science & Technology, Wuhan, China, 430074. E-mail: shengliu63@yahoo.com

For modern LEDs, especially for high-brightness LEDs, both optical extraction and thermal management are critical factors for the high performance of LED packaging. In general, most of the electronic power is converted into heat, and this heat greatly reduces the device's luminosity. In addition, the high junction temperature will shift the peak wavelength of the LED, which will change the color of its light. Narendran and Gu [3] have experimentally demonstrated that the life of LEDs decreases with increasing junction temperature in an exponential manner. Therefore, a low operation temperature is essential for LEDs. Because the market demands that LEDs have high power and packaging density, there is a contradiction between power density and operation temperature, especially when applications require LEDs to operate at full power to obtain the desired brightness.

To address the thermal problem of LEDs, Arik and Weaver [4] carried out a numerical study to understand the chip temperature profile due to bump defects. Finite element techniques were utilized to evaluate the effects of localized hot spots at the active layer of chip. Sano et al. [5] introduced an ultra-bright LED module with excellent heat dissipation characteristics. The

module consists of an aluminum substrate circuit board with outstanding thermal conductivity and workability, with the mount for the LED chips being formed into fine cavities with high reflectance to improve light recovery efficiency. Furthermore, the condenser of this LED module is filled with high-refraction resin on the basis of optical simulation. An improvement in luminance of 25% or more was reported. Petroski [6] developed an LED-based spot module heat sink in a free convective cooling system. A cylindrical tube longitudinal fin (CTLF) heat sink was used to solve the orientation problem of LEDs. Chen et al. [7] presented a silicon-based thermoelectric (TE) for cooling of high power LEDs. The test results show that their TE device can effectively reduce the operation temperature of high power LEDs. Hsu et al. [8] reported a metallic bonding method for LED packaging to provide good thermal dissipation and ohmic contact. Zhang et al. [9] used multi-walled carbon nanotube and carbon black to improve the thermal performance of thermal interface materials (TIM) in high-brightness LED packaging. Tests showed that these materials could effectively decrease the thermal resistance. Acikalin et al. [10] used piezoelectric fans to cool LEDs. Their results showed that the fans could reduce the heat source temperature by as much as 37.4°C. Piezoelectric fans have been shown to be a viable solution for the thermal management of electronic components and LEDs.

Recently, Liu's group began to compare the different cooling technology, including a primitive prototype of the microjet array [11]. The results demonstrated the advantages of the microjet array as compared to the heat pipe and regular fin-based cooling techniques. In their experiments, the temperature was measured by an infrared thermometer, but only the LED surface temperature was obtained, which is far from the junction temperature of LED chips.

In this paper, an enhanced version of the closed microjet array cooling system is proposed to realize the thermal management for high power density LEDs, in particular for LED arrays. In the new system, a very small heat exchanger is used for heat transfer between the system and the environment. An experimental investigation was conducted to test the effectiveness of the proposed system. To achieve a relatively exact temperature distribution in the LEDs, thermocouples were packaged into the LEDs and used for temperature measurement and the evaluation of the cooling effect. Comparative experiments demonstrated that the proposed system is effective. A numerical simulation was also conducted to analyze the flow and temperature distribution inside the microjet device.

MICROJET ARRAY COOLING SYSTEM

Figure 1 illustrates the proposed closed loop LED cooling system. It is composed of three parts: a microjet array device, a micropump, and a mini fluid container with a heat sink. When the LED needs to be cooled, the system is activated. Water or other fluids or gases in the closed loop system are driven into the microjet array device through an inlet by a micropump. Many microjets will form inside the jet device, which are directly impinged onto the bottom plate of the LED array. Because the impinging jet has a very high heat transfer coefficient, the heat created by the LEDs is easily removed by the recycling fluid in the system. The fluid is heated, and its temperature increases after flowing out of the jet device, and then the heated fluid enters into the mini fluid container. The heat sink, which has a fan on the fluid container, will cool the fluid, and the heat will dissipate into the external environment. The cooled fluid is delivered into the jet device to cool the LED array, again driven by the force of the micropump in the system. The above processes constitute one operation cycle of the total system. It should be noted here that the real size of the proposed system can be designed as one small package according to the requirements of the application.

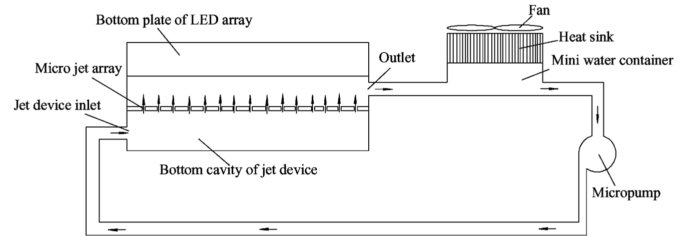

Figure 1 Proposed closed-loop microjet array cooling system.

Figure 2 shows the structure of the jet device of Figure 1 in detail. It consists of several layers, which are (from top to bottom) the chip array layer, the top plate of the jet cavity, the impinging jet cavity, the microjet array layer, and the bottom cavity. Cooled fluid enters into the device through the inlet, which is open at one side of the bottom cavity layer. The fluid flows through the microjet array and forms many microjets, as shown in Figure 2. With sufficient driving force, the jets will impinge onto the top plate of the jet cavity, which is bonded with the chip substrate of the LEDs. The heat conducted into the top plate of the jet cavity through the LED chips will dissipate into the cooled fluid quickly due to the high heat transfer efficiency of the impinging jet. The fluid temperature increases, and the heated fluid flows out from the jet array outlet, which is open at one side of the

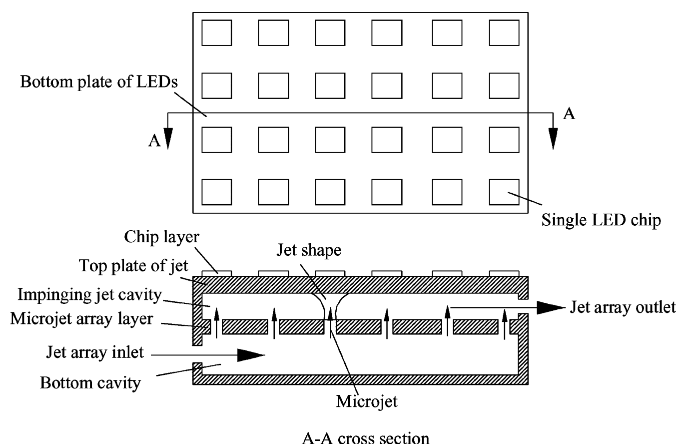

Figure 2 Microjet array device.

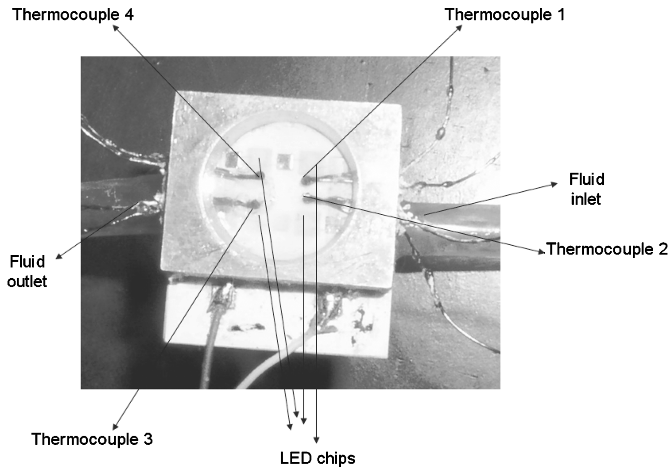

Figure 3 Tested LED array packaged with thermocouples.

top jet cavity layer. Through this process, the heat from the LED chips will be transferred into the fluid efficiently.

The system relies on an impinging jet to transfer heat, which has been demonstrated as a good cooling solution in many applications [12, 13]. Therefore, the most distinguishing advantage of the present concept is its high heat transfer efficiency. In addition, the proposed system is compatible with and easily incorporated into LED packaging structures. It is therefore possible to simplify the package structure and reduce the thermal path, as the impingement is performed on the package substrate.

TEMPERATURE MEASUREMENT AND EXPERIMENTAL SETUP

Temperature Measurement and LED Chip Array

Figure 3 shows one 2 × 2 LED package with four thermocouples embedded inside the module. It is difficult to test the LED junction temperature directly by thermocouples. The objective of these experiments was to check the cooling ability of the proposed system; the exact measurement of the LED junction

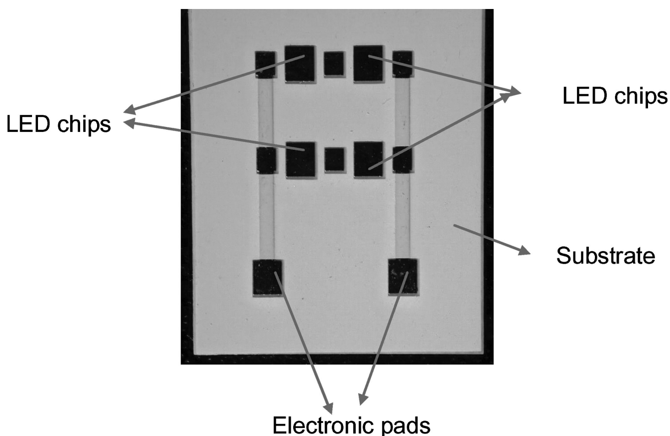

Figure 4 Photo of LED chip layout in the present experiment.

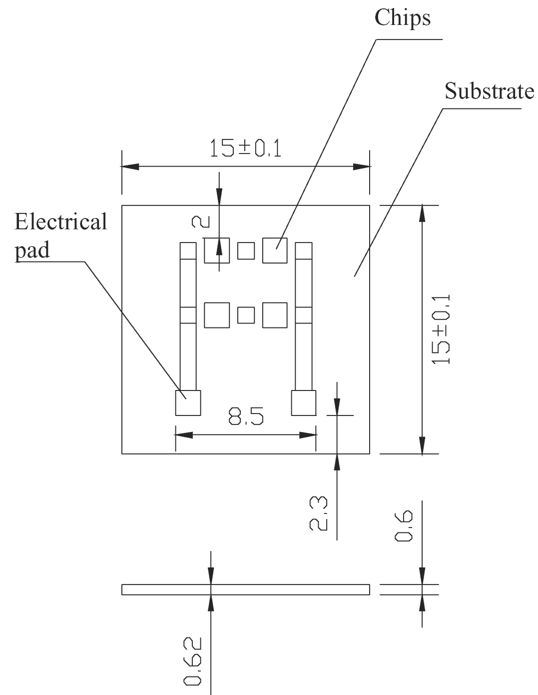

Figure 5 Details of LED chip layout on the substrate. (All dimensions are in mm.)

temperature is not the focus of this paper. Based on this point, four thermocouples were packaged into an LED device, located inside the packaging resin and very close to the LED chips. The distance between the LED chips and thermocouples was about 0.8 mm. According to this LED packaging technique, the temperatures achieved by these thermocouples could indicate the order of magnitude of the LED junction temperature.

Figure 4 demonstrates the chip distribution of the 2 × 2 LED chip array used in the experiments. The four LED chips were distributed on a substrate. Every two chips were connected in a series, and then they were connected in parallel with each other. The size of each LED chip was 1 mm × 1 mm. The substrate size was 15 mm × 15 mm. The details of the LED chip layout on the substrate are given in Figure 5.

Experimental Setup

The experiment system was constructed as shown in Figure 6, and was nearly the same as the one shown in Figure 1. The micropump used in the experiments was based on the electromagnetic principle and was custom-designed and built locally in China. Its maximum power consumption was about 2.16 W. The length, width, and height of the micropump were 6.15 cm, 3.6 cm, and 6.6 cm, respectively. The radiator was purchased from a commercial electronics market, and its length, width, and thickness were 12 cm, 12 cm, and 2.5 cm, respectively. The maximum power consumption of the fan was about 3.6 W. The rotation velocity of the radiator fan was about 2400 rpm. Because the heat transfer efficiency of the microjet device was the

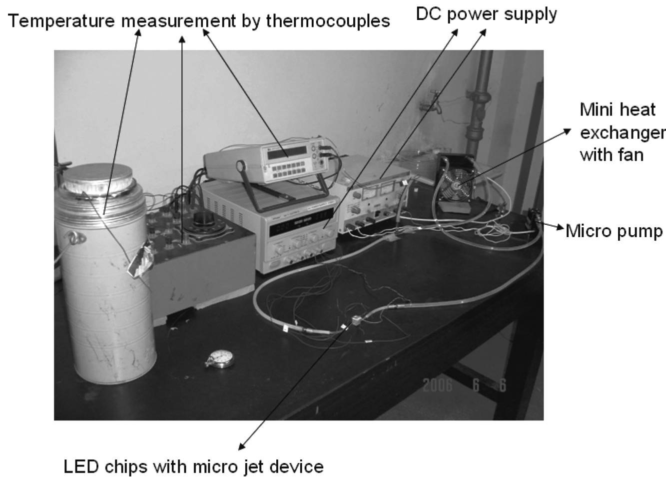

Figure 6 Experimental setup.

focus of our experiment, the sizes of the radiator and micropump were relatively large. In actual applications, they should be smaller in order to save volume and power. The working media of the system was water, and the flow rate of the micropump was adjustable with the input power, at default input power, is 9.7 mL/s. For the microjet device in the present experiment, there were 16 microjets distributed inside, and the diameter of each jet was 0.5 mm. Figure 7 shows the details of the top cavity of the microjet device used in the experiments. It should be noted that the size of the bottom cavity was the same as that of the top cavity.

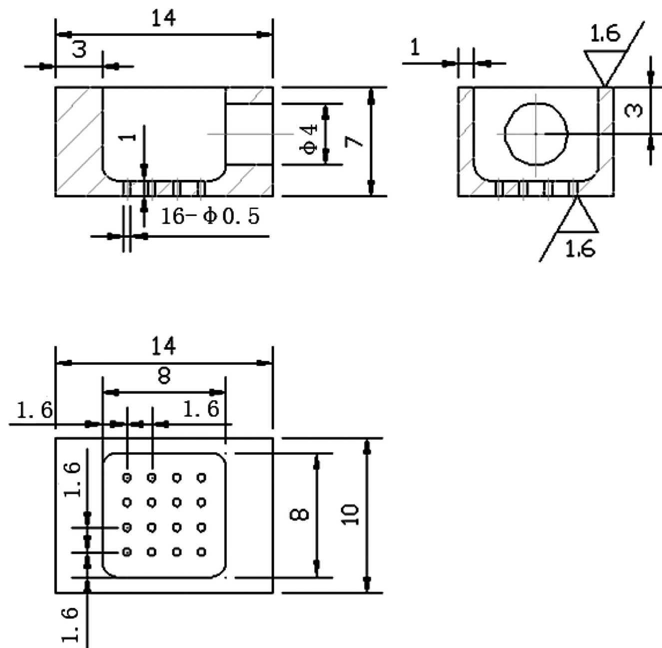

Figure 7 Details of top cavity of microjet device used in the present experiments. (All dimensions are in mm.)

Accuracy Analysis

In the experiments, the temperature was the main parameter for system evaluation, and it was directly measured by thermocouples. Because there were no other indirectly measured parameters, the errors associated with this experiment mainly comprised measurement error of the thermocouples and reading error of the digital multimeter.

Standard T-type thermocouples (Cu-CuNi) were used in the experiments. The cold junction of thermocouples was an ice/water mixture at 0°C. To avoid the possibility that the mineral impurities in the water would change the freezing point of the water, the ice was made from distilled water. The ice bath was put into a vacuum flask to maintain a constant temperature for a long time. Therefore, the error produced in the cold junction reference was negligible. For the thermocouples, at the temperature range from −30°C to 150°C, the measurement error was about 0.2°C. The digital multimeter used was an HP 3468A, with a reading error of 0.01°C. Therefore, the total error of the temperature measurement for the experiments was about 0.21°C.

RESULTS AND ANALYSIS

Estimation of Difference between Measured Temperature and Junction Temperature

The microjet device is the key part of the proposed cooling system, and its cooling performance determines the cooling effect of the total system. As shown in Figure 2, the device is small, and the impinging jets are in a closed space. Therefore, the sensor distribution and measurement were difficult to implement without sophisticated microsensors. Numerical simulation was an effective way to understand and optimize the flow and temperature distribution in the microjet device. Based on the experimental system and microjet device that was fabricated in-house, numerical models were constructed; a typical one is shown in Figures 8 and 9. Figure 9 illustrates the three-dimensional structure

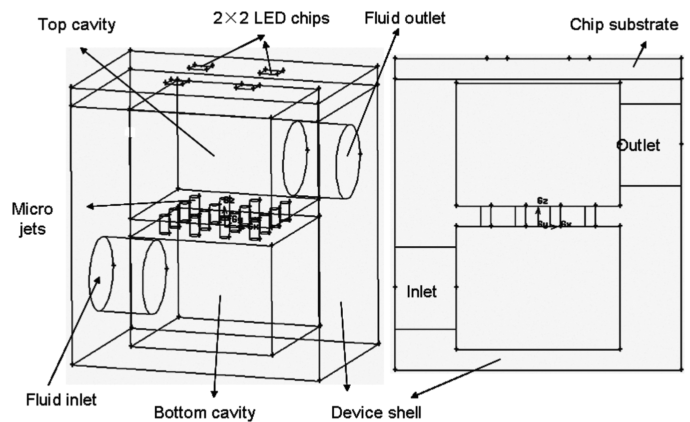

Figure 8 Simulation model.

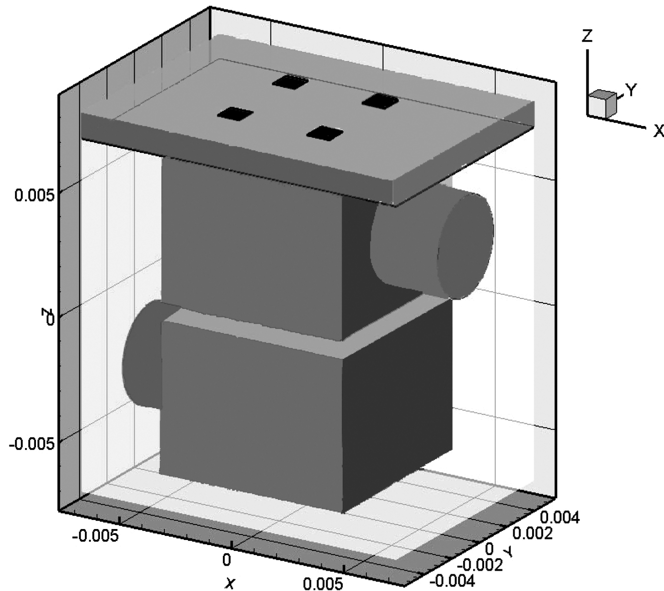

Figure 9 Three-dimensional structure of the proposed model.

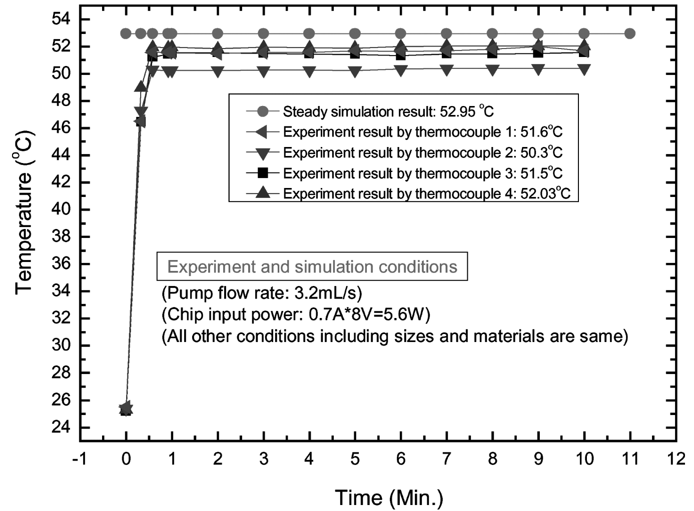

Figure 10 Temperature comparison between experiment and simulation with low pump flow rate.

depicted in Figure 8. Figure 9 shows the inside structure, including the top cavity, bottom cavity, and microjets, after the treatment of translucency and lighting.

As shown in Figure 8, there are several heat transfer passes in the microjet device: LED chips produce heat, and nearly all the heat is transferred to the impinging jet flow by forced convection and to the jet device shell by conduction. For the latter, the heat in the jet device shell exchanges with the environment by natural convection. This model incorporates a coupled heat transfer process that includes natural convection, liquid forced convection, and conduction. Here, the commercial CFD code Fluent 6.2 was used for simulation.

In Figures 8 and 9, the size of the single LED chip was 1 mm $\times$ 1 mm. The other sizes for the microjet device were exactly the same as those in the experiments shown in Figure 7. For the fluid inlet, the boundary condition of constant flow rate was adopted. The turbulence model in the simulation was a standard $k - \varepsilon$ model. A study of the convergence of the grids was conducted before the calculation. The grids were refined until the flow field changed by 0.5%. Finally, 381,889 grids were used in the simulation. The residual control of the continuity equation was 0.001%.

To verify the feasibility of the above model, corresponding experiments were conducted. The working conditions for both the experiments and simulations were exactly the same.

Figure 10 shows a comparison between the temperatures in the experiments and simulations. Here, the pump flow rate was 3.2 mL/s, and the input power of the LEDs was 5.6 W. It can be seen from Figure 10 that the maximum temperature of the LED chips achieved by the steady-state simulation was 52.95°C, and the steady temperatures measured by the four thermocouples were 51.4°C, 52°C, 50.4°C, and 51.9°C. Thus, the temperature difference between the simulation and experimental results measured by the four thermocouples were 1.5°C, 0.95°C, 2.5°C, and 1.05°C. This comparison in Figure 10 shows that the steady temperature achieved by the simulation was slightly higher than that measured in the experiments. This is possible because the maximum temperature of the thermocouples did not reflect the value of the chip temperature. Although the thermocouples were very close to the LED chip, their temperatures were slightly lower than the real chip temperature due to the thermal resistance between the substrate and chip. The real chip temperature was obtained by simulation, as shown in Figure 11. In Figure 11, it can be seen that the maximum temperatures appeared in the positions of the four LED chips. These temperatures can indicate the chip temperature, but they still differ slightly from the junction temperature. Based on the above comparison and analysis, it was found that this model could be used for simulation

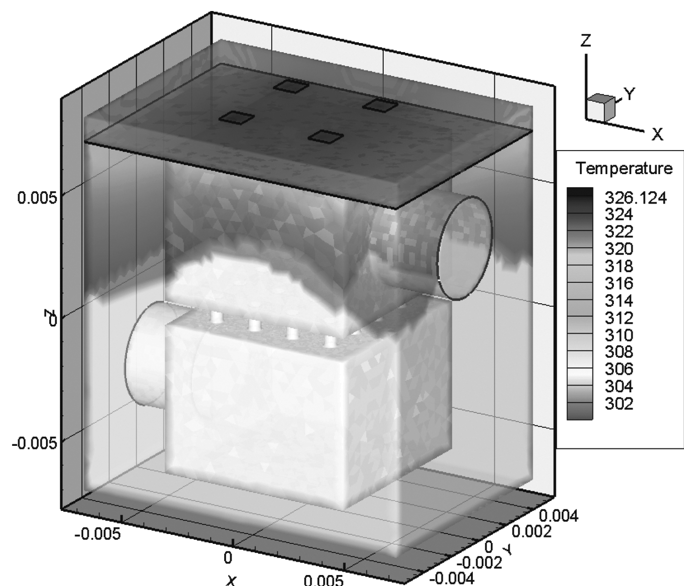

Figure 11 Temperature distribution of microjet device and chip junction by simulation.

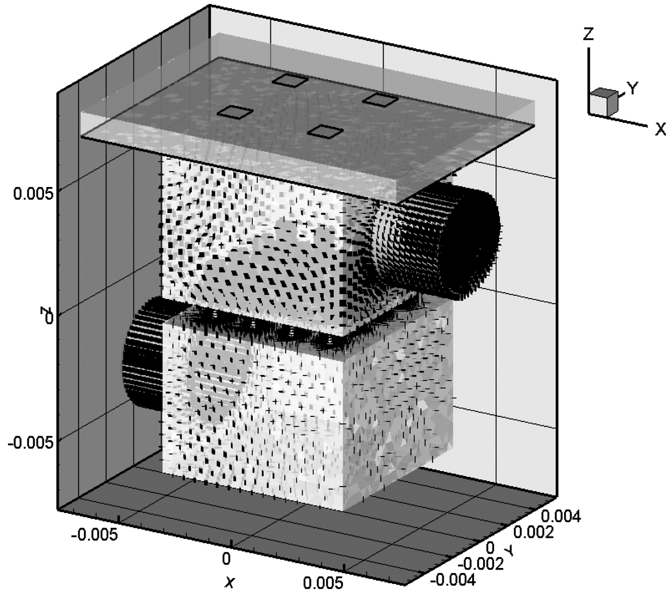

Figure 12 Flow distribution in microjet device shown in Figure 7.

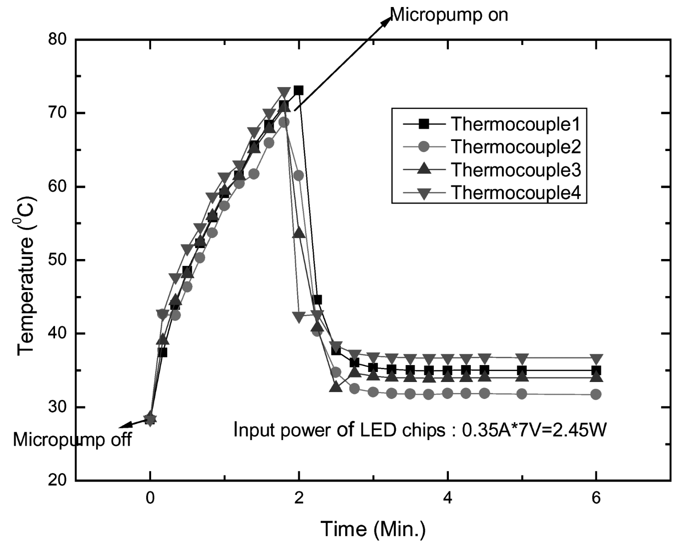

Figure 13 LED temperature variation with time when pump is off and on.

and further optimization, and the measured temperatures in the present experiments can reveal the approximate junction temperature magnitude.

Pressure Drop and Heat Transfer Analysis

The pressure drop and heat transfer coefficients of the proposed microjet device were analyzed according to the above simulation model. Figure 12 shows the flow distribution of the microjet device, and its temperature distribution is illustrated in Figure 11. The simulation conditions were as follows. The flow rate was 3.2 mL/s, and the total input power was 5.6 W. Other simulation dimensions are shown in Figure 7. For the proposed microjet cooling system, the pressure drop in the system is mainly provided by the microjet device.

According to the simulation results shown in Figure 12, the corresponding pressure drop in the microjet device was about 1368 Pa. The heat removed by water was 4.72 W. The average temperature difference between the top cavity ceiling and the water inside the microjet device was 13.352 K. The jet impinging area was about 64E-6 m^2, which was calculated from the data shown in Figure 7. Therefore, based on the equation $Q = hA\Delta T$, the heat transfer coefficient of the impinging microjets was obtained as follows:

$$h = \frac{Q}{A\Delta T} = \frac{4.72}{(64E-6) \times 13.352} W/m^2K$$

$$= 5523.5\ W/m^2K$$

where h is the convection heat transfer coefficient, Q is the heat, A is the heat transfer area, and ΔT is the temperature difference between the top cavity and the water.

LED Temperature Variation under Different Conditions

In the present experiments, the input power was electrical power. Based on our measurements and experience, about 15% of the input electrical power is converted into optical energy. The other 85% of the electrical power generates heat. For the proposed microjet device, its shell has tight contact with the LED substrate; therefore, heat is conducted from the LEDs to the shell of the microjet device. Most of the heat is dissipated into the liquid in the microjet device, and a small portion of the heat is exchanged with the environment by natural convection through the shell surface. The thermal conductivity of the silicone gel on the chips and LED substrate is very low, usually about 0.6 W/mK. In addition, the surface area is small; therefore, the heat transfer into the environment through the top surface of the LED chips is very limited. For the example shown in Figures 10–12, the total input power was 5.6 W, of which 0.8 W was converted into optical energy and 4.8 W was converted into heat. For the 4.8 W heat, 4.72 W is removed by water, and the rest (0.08W) is dissipated into the environment by natural convection through the microjet device shell and the top surface of the LED chips, which are covered by silicone gel and a lens.

Figure 13 shows the variation of the LED temperatures with time. The total input power of the four LED chips was 2.45 W, and the flow rate of the micropump was 9.7 mL/s. In this experiment case, the micropump was designed not to run immediately. After the LED had been lit up for about two minutes, the micropump would begin to run. As shown in Figure 13, the LED temperature measured by thermocouple 4 was the highest of the four thermocouples. When the cooling system was not running, the LED temperature increased very quickly; within two minutes, the temperature measured by thermocouple 4 increased from 28°C to nearly 72°C, and it continued to increase sharply. However, after the micropump had begun to operate, the cooling system was activated, and the temperature measured

by thermocouple 4 decreased from 72°C to 36.7°C within one minute. The contrast clearly demonstrates the cooling performance of the proposed system. As shown in Figure 13, the LEDs reached a steady temperature situation very rapidly because the radiator can dissipate heat into environment quickly. In Figure 13, it should be noted that the four thermocouples display different temperatures. When the LED temperatures reached a steady state, the maximum temperature difference (5°C) was between thermocouple 4 and thermocouple 2. The temperature difference of the four thermocouples in Figure 13 can be attributed to the unequal cooling effect by the microjet device, as every chip received the same input power in the experiments. These differences demonstrate that for the proposed jet device, the temperature uniformity needs to be perfected, and the sizes and distribution of the microjets should be optimized.

Figure 14 shows the variation of LED temperature with time at different LED input power levels with the same micropump flow rate. Here, the micropump flow rate was only 4.5 mL/s. The temperature data was obtained by thermocouple 4. When the input power of the LEDs was 2.52 W, the steady temperature was 36.7°C. However, when the input power was increased to 9.3 W, the LED temperature remained steady at nearly 54°C.

Figure 15 shows the variation of LED temperature with time at different pump flow rates with the same LED input power. Here, the total input current was 350 mA, and the voltage was 7V; thus, the input power of the LED chips was 2.45 W. It can be observed that as the pump flow rate increased, the LED temperature decreased. When the flow rate of the micropump was 3.2 mL/s, the LED temperature measured by thermocouple 4 was nearly 39°C; however, when the flow rate was increased to 9.7 mL/s, the LED temperature decreased to about 33°C. It is easy to explain this phenomenon. When the pump flow rate increases, the heat transfer coefficient of the impinging jet in the microjet device will increase, and thus the heat from the LED chips will be removed more effectively. However, it should be noted that as the pump flow rate is increased, the micropump consumes more power, which increases the operation cost. In real application, there should be some trade-offs in design between the heat transfer efficiency and power consumption.

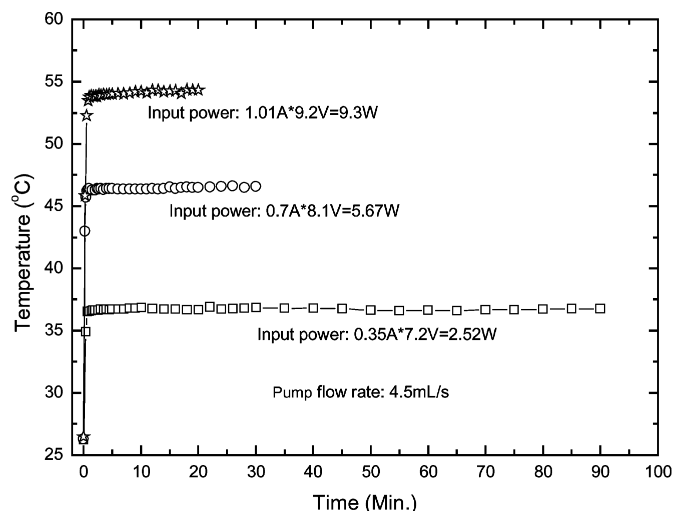

Figure 14 LED temperature variation with time at different LED input powers.

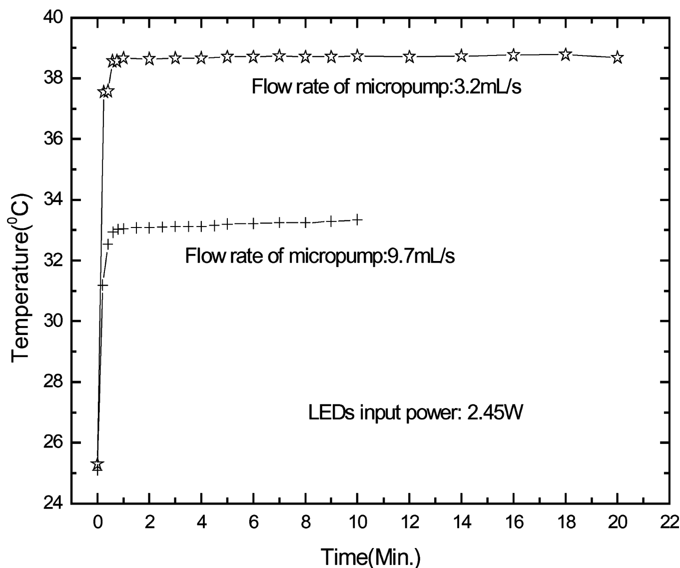

Figure 15 LED temperature variation with time at different pump flow rates.

It is obvious that the design of the microjet device below the LED chips is the key for increasing heat transfer efficiency. However, for the components in this experimental system, no attempt was made to optimize the dimensions, materials, or structures.

SUMMARY

In this paper, an enhanced version of a closed loop microjet cooling system for thermal management of LEDs is presented. To evaluate the cooling performance of the proposed system, four thermocouples were packaged into the LED chips to measure the LED temperature. The experiments demonstrated that the proposed cooling system provides efficient cooling, but the parameters of the microjet array device need to be optimized. Experiments were also conducted to evaluate the cooling effect under different conditions such as different micropump flow rates and different input powers. The results showed that with increasing pump flow rate, the cooling effect was improved. A numerical simulation was also conducted, and the feasibility of the simulation model was proven by comparison with the experimental results. The preliminary numerical results revealed the pressure drop and heat transfer coefficient in the microjet devices.

ACKNOWLEDGMENTS

The authors acknowledge the financial support from the Key Technology R&D Program of Hubei Province, China

(2006AA103A04). The authors also would like to acknowledge Mr. Zetao Ma and Dr. Mingxiang Chen for their valuable discussions and help in experiment preparation. We also want to express our sincere thanks to Prof. A. J. Ghajar of Oklahoma State University for his kind help in editing our paper.

REFERENCES

[1] Zukauskas, A., Shur, M. S., and Gaska, R., *Introduction to Solid-State Lighting,* pp. 21–29, John Wiley & Sons, New York, 2002.

[2] Alan, M., *Solid State Lighting—a World of Expanding Opportunities at LED 2002*, *III–Vs Review*, vol. 16, no. 1, pp. 30–33, 2003.

[3] Narendran, N., and Gu, Y. M., Life of LED-Based White Light Sources, *IEEE Journal of Display Technology*, vol. 1, no. 1, pp. 167–171, 2005.

[4] Arik, M., and Weaver, S., Chip Scale Thermal Management of High Brightness LED Packages, *Fourth International Conference on Solid State Lighting, Proc. SPIE*, vol. 5530, pp. 214–223, Denver, Colorado, 2004.

[5] Sano, S., Murata, H., and Hattori, K., Development of Flat Panel LED Module with Heat Sink, *Mitsubishi Cable Ind. Rev.,* vol. 86, pp. 112–118, 1993.

[6] Petroski, J., Understanding Longitudinal Fin Heat Sink Orientation Sensitivity for Light Emitting Diode (LED) Lighting Applications, *Proc. International Electronic Packaging Technical Conference and Exhibition*, pp. 111–117, Maui, Hawaii, 2003.

[7] Chen, J. H., Liu, C. K., Chao, Y. L., and Tain, R. M., Cooling Performance of Silicon-Based Thermoelectric Device on High Power LED, *Proc. 24th International Conference on Thermoelectrics,* pp. 53–56, Clemson, South Carolina, 2005.

[8] Hsu, C. C., Wang, S. J., and Liu, C. Y., Metallic Wafer and Chip Bonding for LED Packaging, *Proc.* 5th *Pacific Rim Conference on Lasers and Electro-Optics,* vol. 1, p. 26, Taipei, Taiwan, 2003.

[9] Zhang, K., Xiao, G. W., Wong, C. K. Y., Gu, H. W., Yuen, M. M. F., Chan, P. C. H., and Xu, B., Study on Thermal Interface Material with Carbon Nanotubes and Carbon Black in High-Brightness LED Packaging with Flip-Chip, *Proc. 55th Electronic Components and Technology,* pp. 60–65, Orlando, Florida, 2005.

[10] Acikalin, T., Garimella, S. V., Petroski, J., and Arvind, R., Optimal Design of Miniature Piezoelectric Fans for Cooling Light Emitting Diodes, *Proc. Ninth Intersociety Conference on Thermal and Thermomechanical Phenomena in Electronic Systems,* vol. 1, pp. 663–671, New York, 2004.

[11] Liu, S., Lin, T., Luo, X. B., Chen, M. X., and Jiang, X. P., A Microjet Array Cooling System for Thermal Management of Active Radars and High-Brightness LEDs, *Proc. Fifty-Sixth Electronic Components & Technology Conference,* pp. 1634–1638, San Diego, Calif., 2006.

[12] Wu, S., Mai, J., Tai, Y. C., and Ho, C. M., Micro Heat Exchanger by Using MEMS Impinging Jets, *Proc. Twelfth IEEE International Conference on Micro Electro Mechanical Systems*, pp. 171–176, Orlando, Florida, 1999.

[13] Fleischer, A. S., and Nejad, S. R., Jet Impingement Cooling of a Discretely Heated Portion of a Protruding Pedestal with a Single Round Air Jet, *Experimental Thermal and Fluid Science,* vol .28, pp. 893–901, 2004.

Xiaobing Luo is an associate professor in Huazhong University of Science and Technology (HUST), Wuhan, China. He works at the School of Energy and Power Engineering and Wuhan National Lab for Optoelectronics in HUST. He received his Ph.D. in 2002 from Tsinghua Univeristy, China. His main research interests are heat and mass transfer, LED, microfluidics, MEMS, sensors, and actuators. He has published more than 20 papers, and applied for and owned 20 patents in the United States, Korea, Japan, Europe, and China.

Wei Chen is a master's student in Huazhong University of Science and Technology (HUST), Wuhan, China. He works at the School of Energy and Power Engineering in HUST. Currently, he is working on the thermal management of high power LEDs.

Runxia Sun is a master's student in Huazhong University of Science and Technology (HUST), Wuhan, China. She works at the School of Energy and Power Engineering in HUST. Currently, she is working on capillary pump loop and cooling of electronic devices.

Sheng Liu is a specially recruited professor, director of the Institute of Microsystems, and director of MOEMS Division, Wuhan National Lab of Optoelectronics, Huazhong University of Science and Technology, Wuhan, China. He obtained his Ph.D. from Stanford University in 1992. His main research interests are LED, MEMS, IC packaging, mechanics, and sensors. He has published more than 200 technical articles and filed more than 50 patents.